

This is a non-peer reviewed preprint submitted to
EarthArXiv



Subsequent peer-reviewed versions of this manuscript may have slightly different content. The authors welcome feedback.

[†]Corresponding email address: sandy.herho@email.ucr.edu

Consecutive Dry Days as a Scale-Dependent Predictor of Tropical Peatland Fire Occurrence in Indonesia

Rusmawan Suwarman¹, Raffly Azaria¹, Sandy H. S. Herho^{2,3,4*},
Edvin Aldrian⁵

¹Atmospheric Science Research Group, Bandung Institute of Technology
(ITB), Jalan Ganesha 10, Bandung, 40132, West Java, Indonesia.

^{2*}Department of Earth and Planetary Sciences, University of California,
900 University Ave., Riverside, 92521, CA, USA.

³Applied and Environmental Oceanography Research Group, Bandung
Institute of Technology (ITB), Jalan Ganesha 10, Bandung, 40132, West
Java, Indonesia.

⁴Samudera Sains Teknologi (SST) Ltd., Gang Sarimanah XIII/67,
Bandung, 40151, West Java, Indonesia.

⁵Research Center for Climate and Atmosphere (PRIMA), National
Research and Innovation Agency (BRIN), Jalan Dr. Djundjuran 133,
Bandung, 40173, West Java, Indonesia.

*Corresponding author(s). E-mail(s): sandy.herho@email.ucr.edu;

Abstract

Tropical peatland fires in Indonesia generate severe environmental, health, and economic impacts, yet current fire prediction systems exhibit scale-dependent limitations. This study investigates the relationship between Consecutive Dry Days (CDD) indices and fire occurrence across multiple spatial scales in South Sumatra and West Kalimantan provinces (2015-2019). Using hierarchical buffer analysis (25, 50, 100, 150 km radii) around meteorological stations, we analyzed MODIS hotspot data with >80% confidence against CDD classifications. Maximum CDD values reached 41 days (South Sumatra) and 27 days (West Kalimantan) during the 2015 El Niño event. Correlation analysis revealed pronounced scale dependency, with optimal meteorological station representativeness at 50 km radius ($r = 0.776-0.821$, $p < 0.01$). Weak negative correlations at 25 km radii reflect urban bias in station placement, while correlations degraded

beyond 100 km due to atmospheric boundary layer constraints. Hotspot frequencies increased exponentially with CDD duration, particularly on peatlands where very long droughts (>30 days) generated 156.2 ± 34.7 hotspots per event. These findings indicate current meteorological networks inadequately sample fire-prone landscapes, suggesting strategic station deployment at 50 km intervals could substantially improve early warning systems across Southeast Asia’s vulnerable peatland regions.

Keywords: atmospheric boundary layer, drought index, fire prediction, peatland combustion, spatial scale

1 Introduction

Tropical peatland fires represent one of the most significant yet poorly constrained components of the global carbon cycle, with Indonesian fires alone contributing a substantial fraction of global fire carbon emissions during extreme events (van der Werf et al., 2017). The 2015 El Niño-induced fires in Indonesia released carbon dioxide equivalent exceeding the annual fossil fuel emissions of major industrialized nations, creating atmospheric perturbations detectable at global monitoring stations (Huijnen et al., 2016). During peak burning periods, daily emissions surpassed those of entire economic blocs, while particulate matter concentrations reached hazardous levels across a region spanning thousands of kilometers (Kiely et al., 2021). These emissions create a positive feedback loop with climate change, as increased atmospheric CO₂ enhances drought severity through regional warming and altered precipitation patterns, which in turn promotes more extensive fires (Tian et al., 2011).

The economic and public health impacts of tropical peatland fires extend far beyond their climate effects, creating cascading consequences across multiple sectors and nations. The 2015 Indonesian fires caused economic losses representing a significant fraction of national GDP, with damages distributed across carbon emissions costs, land-cover degradation, and health impacts (Kiely et al., 2021). This comprehensive assessment substantially exceeds earlier estimates by incorporating long-term health effects and ecosystem service losses previously unquantified. The transboundary nature of fire impacts manifested in substantial losses for neighboring countries, demonstrating how localized burning creates regional economic disruption (Sheldon and Sankaran, 2017).

Health impacts represent a particularly severe dimension of fire consequences, with smoke exposure from the 2015 fires resulting in widespread premature mortality across Southeast Asia (Marlier et al., 2015). The fine particulate matter generated by peat combustion penetrates deep into human lungs, causing acute respiratory infections, exacerbating chronic conditions, and triggering cardiovascular events (Edwards et al., 2020). Children and elderly populations experienced disproportionate impacts, with pediatric respiratory hospitalizations increasing dramatically in affected regions during peak haze periods (Hein et al., 2022).

72 Despite these severe impacts, current fire prediction systems exhibit fundamental
73 limitations in tropical peatland environments, where unique hydrological processes and
74 combustion dynamics differ markedly from the temperate and boreal systems for which
75 most indices were developed (Taufik et al., 2017). The Canadian Fire Weather Index
76 System, widely adopted globally, fails to account for the critical role of groundwater
77 depth in controlling peat ignitability, while the Keetch-Byram Drought Index underes-
78 timates moisture deficits in organic soils with high water-holding capacity (Kudláčková
79 et al., 2024). These systemic inadequacies result in delayed warnings, misallocated
80 suppression resources, and preventable damages to communities and ecosystems.

81 The challenge of predicting tropical fire occurrence stems partly from inadequate
82 understanding of scale-dependent relationships between meteorological observations
83 and fire activity. While weather stations provide point measurements of atmo-
84 spheric conditions, fires respond to spatially integrated drought patterns influenced by
85 atmospheric boundary layer (ABL) dynamics, mesoscale circulations, and landscape
86 heterogeneity (Linn et al., 2025). The planetary boundary layer in tropical regions
87 exhibits distinct characteristics—including strong diurnal cycles, frequent convective
88 activity, and complex land-sea interactions—that modulate the spatial coherence of
89 meteorological conditions (Zheng et al., 2023). The representative radius of meteo-
90 rological stations—the spatial extent over which their measurements correlate with
91 fire occurrence—remains poorly quantified despite its fundamental importance for
92 operational fire warning systems (Vitolo et al., 2020).

93 Consecutive Dry Days (CDD) indices have emerged as promising predictors of
94 fire danger in water-limited ecosystems, offering advantages over instantaneous mete-
95 orological variables by capturing cumulative moisture stress (O et al., 2020). The
96 mechanistic relationship between precipitation deficits and fire occurrence operates
97 through multiple pathways: direct desiccation of surface fuels, lowering of groundwa-
98 ter tables that expose deeper peat layers, and physiological stress on vegetation that
99 increases dead fuel loads (Dadap et al., 2019). Unlike conventional fire weather indices
100 that emphasize atmospheric vapor pressure deficits and wind speed, CDD directly
101 quantifies the precipitation deficits that control peat moisture content—the primary
102 determinant of tropical peat ignitability below critical moisture thresholds (Usup et al.,
103 2004).

104 However, fundamental knowledge gaps persist in applying CDD indices to tropical
105 fire prediction. The precipitation threshold defining a "dry day"—commonly set at a
106 minimal value—derives from agricultural applications focused on crop water require-
107 ments rather than fire-specific calibration (Bohlmann and Laine, 2024). This arbitrary
108 threshold may poorly represent the minimum precipitation needed to maintain peat
109 moisture above ignition thresholds, particularly given the high evapotranspiration
110 rates characteristic of tropical environments (Hirano et al., 2015). Furthermore, the
111 relationship between surface precipitation and peat moisture involves complex inter-
112 actions with canopy interception, preferential flow pathways, and lateral groundwater
113 movement that simple threshold approaches cannot capture.

114 Indonesia’s fire-prone provinces of South Sumatra and West Kalimantan exem-
115 plify the convergence of biophysical and anthropogenic factors that make tropical fire

116 prediction particularly challenging. These regions contain extensive degraded peat-
117 lands where decades of canal construction for agriculture and timber extraction have
118 substantially lowered water tables, creating conditions conducive to deep smoldering
119 combustion (Konecny et al., 2016). The interaction between drainage infrastructure
120 and natural hydrology creates heterogeneous moisture patterns that vary at scales
121 from meters to kilometers, complicating the extrapolation of point-based meteorolog-
122 ical measurements to landscape-scale fire risk (Yokelson et al., 2022). During recent
123 El Niño events, these provinces experienced severe burning, yet fire occurrence exhib-
124 ited high spatial variability that current prediction systems failed to capture, with
125 some drained areas burning extensively while adjacent undrained forests remained
126 unaffected (Grosvenor et al., 2024).

127 The El Niño-Southern Oscillation (ENSO) modulates Indonesian precipitation
128 through well-established teleconnections involving Walker circulation disruption and
129 Indo-Pacific sea surface temperature anomalies (Hu et al., 2025). During El Niño
130 events, anomalous subsidence over the Maritime Continent suppresses convective pre-
131 cipitation, extending dry seasons substantially and creating windows of extreme fire
132 risk (Pan et al., 2018). However, the translation of these regional climate anoma-
133 lies to local fire occurrence depends critically on processes operating across multiple
134 spatial scales, from synoptic atmospheric patterns through mesoscale circulations to
135 microtopographic variations in peat depth and drainage (Cobb et al., 2017). Previ-
136 ous studies have examined either large-scale climate drivers or local fuel conditions in
137 isolation, but the intermediate scales at which meteorological measurements become
138 representative of fire danger remain unexplored, creating a critical gap in multi-scale
139 fire prediction frameworks.

140 This study addresses these critical knowledge gaps by systematically evaluating
141 the relationship between CDD indices and fire occurrence across multiple spatial
142 scales in South Sumatra and West Kalimantan provinces. Specifically, we test the
143 hypothesis that meteorological station representativeness for fire prediction follows a
144 scale-dependent pattern related to ABL processes and landscape characteristics. By
145 analyzing half a decade of drought and fire data encompassing major El Niño events
146 at multiple buffer distances from weather stations, we aim to: (1) quantify the optimal
147 spatial scale for drought-fire correlations in tropical peatlands; (2) evaluate the effec-
148 tiveness of CDD as a fire predictor compared to instantaneous meteorological variables;
149 (3) identify the meteorological and landscape factors controlling the spatial coherence
150 of fire danger; and (4) provide evidence-based recommendations for fire monitoring
151 network design in tropical regions. Our findings have direct implications for improving
152 early warning systems across Southeast Asia and other tropical regions where lim-
153 ited meteorological infrastructure must serve vast fire-prone landscapes, potentially
154 preventing future disasters comparable to those experienced during recent El Niño
155 events.

2 Materials and Methods

2.1 Study Area and Data Sources

The study encompasses two provinces in Indonesia characterized by extensive tropical peatland systems and pronounced fire vulnerability: South Sumatra ($\mathcal{A}_{\text{SS}} = 3.41 \times 10^6$ ha) and West Kalimantan ($\mathcal{A}_{\text{WK}} = 8.39 \times 10^6$ ha). These regions contain substantial peatland distributions with areas $\mathcal{A}_{\text{peat,SS}} = 9.21 \times 10^5$ ha and $\mathcal{A}_{\text{peat,WK}} = 1.54 \times 10^6$ ha, respectively (Tangang et al., 2017). The selection of these provinces is motivated by their unique fire dynamics, where smoldering peat combustion operates at temperatures of 500-700°C and can persist underground for weeks despite surface rainfall (Graham et al., 2022; Crawford et al., 2024).

The spatial domain $\Omega \subset \mathbb{R}^2$ is bounded by geographic coordinates $\phi \in [-5.0^\circ, 2.0^\circ]$ and $\lambda \in [102.0^\circ, 114.0^\circ]$, encompassing regions where ENSO teleconnections create predictable drought-fire patterns through Walker circulation disruption (Pan et al., 2018). The mechanistic pathway involves anomalous sinking air over Indonesia during El Niño events, with Eastern Pacific events causing nearly double the fire emissions of Central Pacific events due to stronger circulation anomalies (Field et al., 2016). Figure 1 illustrates the spatial distribution of meteorological stations and forest coverage across both provinces.

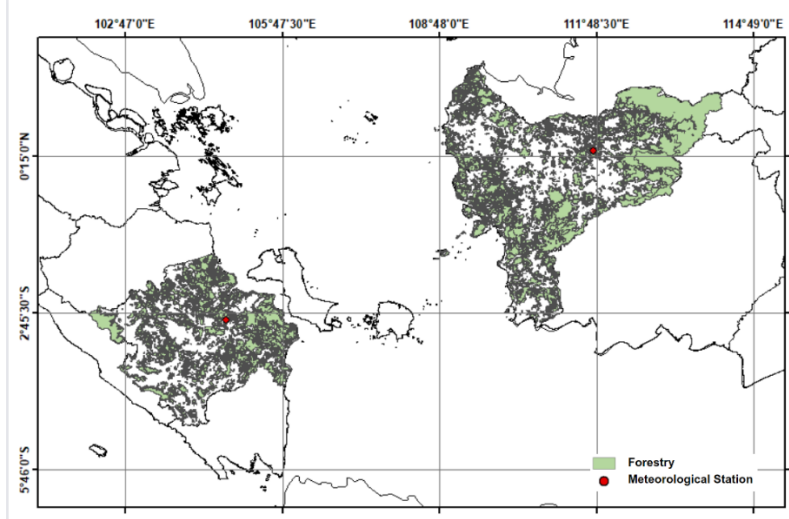


Fig. 1 Spatial distribution of study regions showing meteorological stations and forest coverage across South Sumatra and West Kalimantan provinces, overlaid on peatland distribution maps.

Ground-based meteorological observations $\mathbf{P} = \{P_t : t \in \mathcal{T}\}$ and satellite-derived hotspot data $\mathbf{H} = \{H_t : t \in \mathcal{T}\}$ were acquired for the temporal domain $\mathcal{T} = [t_0, t_f]$, where t_0 = January 1, 2015 and t_f = December 31, 2019. This period encompasses the 2015 El Niño event, which caused Indonesia’s most severe fires since 1997, releasing massive quantities of CO_2 with daily emissions exceeding the entire European Union’s

179 fossil fuel output (Kiely et al., 2021). Daily precipitation measurements were obtained
 180 from BMKG stations located at $\mathbf{s}_1 = (104.7^\circ\text{E}, 2.9^\circ\text{S})$ in South Sumatra and $\mathbf{s}_2 =$
 181 $(111.5^\circ\text{E}, 0.15^\circ\text{S})$ in West Kalimantan.

182 MODIS-derived hotspot data satisfying the confidence threshold $\kappa > 0.8$ were
 183 utilized following extensive validation studies in tropical forests (Giglio et al., 2016).
 184 The confidence metric emerges from brightness temperature anomaly tests:

$$\kappa = f(T_4, T_{11}, \Delta T_{4,11}, \sigma_{bg}), \quad (1)$$

185 where T_4 and T_{11} represent brightness temperatures at 4 μm and 11 μm channels,
 186 $\Delta T_{4,11} = T_4 - T_{11}$, and σ_{bg} denotes background variability. The 80% threshold balances
 187 commission errors from forest clearings (16% in tropical forests) against omission errors
 188 for understory fires obscured by dense canopies (Csiszar et al., 2006).

189 2.2 Consecutive Dry Days Index and Spatial Analysis

190 Let $\mathcal{P} = \{P_i\}_{i=1}^N$ represent the daily precipitation time series, where $N = |\mathcal{T}|$ denotes
 191 the total observation days. The CDD index quantifies drought persistence through the
 192 operator (Duan et al., 2017):

$$\Xi_j = \max_{\substack{i \in \mathcal{I}_j \\ i+n \leq N}} \left\{ n \in \mathbb{N} : \bigwedge_{k=0}^{n-1} \mathbb{I}(P_{i+k} < \tau) = 1 \right\}, \quad (2)$$

193 where \mathcal{I}_j represents the index set for period j , and $\mathbb{I}(\cdot)$ denotes the indicator func-
 194 tion. The precipitation threshold $\tau = 1 \text{ mm day}^{-1}$ follows ETCCDI standards (Zwiers
 195 and Zhang, 2009), though we acknowledge the absence of peer-reviewed validation for
 196 this specific threshold in tropical fire contexts (Chen et al., 2014). The mechanistic
 197 justification for drought thresholds in fire-prone ecosystems relates to soil moisture
 198 depletion rates and vegetation stress responses, with peatland systems exhibiting criti-
 199 cal moisture thresholds of 200-400% (dry weight basis) for ignition (Mortelmans et al.,
 200 2024).

201 The Indonesian BMKG classification categorizes CDD values based on empirical
 202 observations of drought impacts on agricultural and forest systems:

$$\Psi(\Xi) = \begin{cases} \text{Very short} & \text{if } 1 \leq \Xi \leq 5 \\ \text{Short} & \text{if } 6 \leq \Xi \leq 10 \\ \text{Moderate} & \text{if } 11 \leq \Xi \leq 20 \\ \text{Long} & \text{if } 21 \leq \Xi \leq 30 \\ \text{Very long} & \text{if } \Xi > 30 \end{cases} \quad (3)$$

203 This classification aligns with field observations showing nonlinear fire responses to
 204 drought duration, where peat fires exhibit threshold behavior once water tables drop
 205 below 40-60 cm (Gaveau et al., 2014).

206 To investigate scale-dependent relationships between meteorological observations
 207 and fire occurrence, we implemented a hierarchical buffer analysis using ArcGIS 10.8.

208 The theoretical foundation rests on ABL dynamics, where the planetary boundary
 209 layer height (typically 0.3-3 km in tropical regions) fundamentally determines mete-
 210 orological representativeness (Werth et al., 2011). Let $\mathbf{s} \in \Omega$ denote a meteorological
 211 station location. The circular buffer zone $\mathcal{B}_r(\mathbf{s})$ at radius r is defined through the
 212 Euclidean distance metric:

$$\mathcal{B}_r(\mathbf{s}) = \{\mathbf{x} \in \Omega : \|\mathbf{x} - \mathbf{s}\|_2 \leq r\}, \quad (4)$$

213 where $\|\cdot\|_2$ represents the Euclidean norm. The multi-scale analysis employs radii
 214 $\mathbf{r} = \{r_1, r_2, r_3, r_4\} = \{25, 50, 100, 150\}$ km, generating nested buffer zones satisfying
 215 $\mathcal{B}_{r_i}(\mathbf{s}) \subseteq \mathcal{B}_{r_j}(\mathbf{s})$ for $i < j$.

216 The spatial coherence of meteorological conditions follows exponential decay based
 217 on turbulence theory (Stull, 1988):

$$\mathcal{R}(r) = \mathcal{R}_0 \exp\left(-\frac{r}{\Lambda}\right), \quad (5)$$

218 where \mathcal{R}_0 represents the autocorrelation at the origin and Λ denotes the decorrela-
 219 tion length scale, typically 2-5 times the ABL height. Diurnal variations in boundary
 220 layer structure create temporal variations in Λ , with convective daytime conditions
 221 enabling greater spatial coherence (1-2 km mixed layer) compared to stable nocturnal
 222 stratification (Kopplitz et al., 2018).

223 The hotspot count within each buffer zone is computed through the spatial integral:

$$H_{k,r} = \int_{\mathcal{B}_r(\mathbf{s})} \sum_{t \in \mathcal{T}_k} h(\mathbf{x}, t) d\mathbf{x}, \quad (6)$$

224 where $h(\mathbf{x}, t)$ represents the hotspot density function and $\mathcal{T}_k = \{t : \Psi(\Xi_t) = k\}$
 225 denotes the temporal subset corresponding to CDD class k as defined in Equation (3).
 226 In practice, this integral is approximated using the Spatial Join operation in ArcGIS
 227 through point-in-polygon containment tests based on the computational geometry
 228 algorithm of Ma et al. (2018).

229 2.3 Statistical Framework and Normalization

230 The normalized hotspot ratio compensates for varying drought frequency across
 231 classes, addressing the spatial autocorrelation inherent in fire occurrence patterns
 232 (Bataineh et al., 2006). For CDD class $k \in \mathcal{C}$ and radius r , we define:

$$\varrho_{k,r} = \frac{H_{k,r}}{|\mathcal{T}_k|}, \quad (7)$$

233 where $|\mathcal{T}_k|$ represents the cardinality of the temporal subset and $H_{k,r}$ is computed using
 234 Equation (6). This normalization accounts for the observation that longer drought
 235 periods naturally occur less frequently, preventing bias toward extreme events (Chen
 236 et al., 2014).

237 The correlation structure between CDD values and hotspot ratios is quantified
 238 through Pearson’s product-moment correlation coefficient, justified by the Central
 239 Limit Theorem despite the non-normal distribution of fire occurrence data (Havlicek
 240 and Peterson, 1976). We apply logarithmic transformation to fire counts, converting
 241 multiplicative processes to additive ones suitable for linear analysis:

$$\rho_r = \frac{\mathbb{E}[(X - \mu_X)(Y_r - \mu_{Y_r})]}{\sigma_X \sigma_{Y_r}}, \quad (8)$$

242 where X represents CDD values computed from Equation (2) and $Y_r = \log(\varrho_{k,r} + 1)$
 243 denotes log-transformed hotspot ratios at radius r . The sample estimate is computed
 244 as:

$$\hat{\rho}_r = \frac{\sum_{i=1}^n (x_i - \bar{x})(y_{r,i} - \bar{y}_r)}{\sqrt{\sum_{i=1}^n (x_i - \bar{x})^2} \sqrt{\sum_{i=1}^n (y_{r,i} - \bar{y}_r)^2}}. \quad (9)$$

245 Statistical significance is assessed through the t -transformation under the null
 246 hypothesis $\mathcal{H}_0 : \rho = 0$:

$$T = \hat{\rho}_r \sqrt{\frac{n-2}{1 - \hat{\rho}_r^2}} \sim t_{n-2}, \quad (10)$$

247 which follows a Student’s t -distribution with $\nu = n - 2$ degrees of freedom. The test
 248 statistic accounts for the reduction in degrees of freedom due to parameter estimation
 249 (Squire et al., 2021). All statistical computations were performed using Microsoft
 250 Excel’s Data Analysis ToolPak, with correlation matrices computed for each buffer
 251 radius and significance levels evaluated at $\alpha \in \{0.01, 0.05\}$ following standard practice
 252 in fire-climate studies (Sun et al., 2024).

253 3 Results and Discussion

254 Drought severity varied dramatically between provinces during 2015-2019. South
 255 Sumatra recorded maximum CDD of 41 days during the September-October 2015 El
 256 Niño event, while West Kalimantan peaked at 27 days in August-September 2015.
 257 This 2015 event triggered Indonesia’s worst fires since 1997 (Field et al., 2016). The
 258 timing matters—Taufik et al. (2022) identified critical moisture thresholds in peat-
 259 lands where ignition becomes likely after extended dry periods, explaining why South
 260 Sumatra’s longer droughts produced more severe burning.

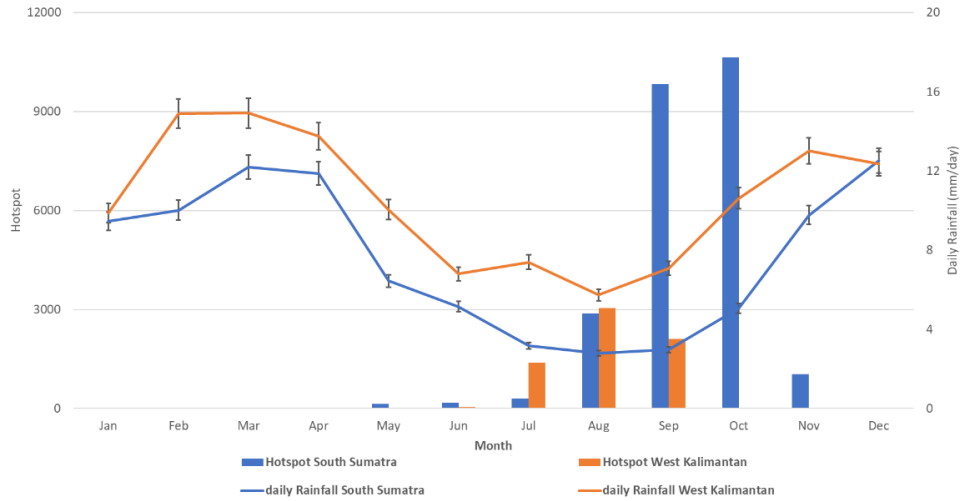


Fig. 2 Climatological monthly rainfall patterns and hotspot occurrences for South Sumatra and West Kalimantan (2015-2019). Error bars represent standard deviation of monthly rainfall, while bars indicate total monthly hotspot counts.

Rainfall and fire showed the expected inverse relationship (Figure 2). South Sumatra's monsoonal climate drove peak burning in August-October, while West Kalimantan's equatorial rainfall pattern pushed maximum fire activity into July-September. These provincial patterns strengthen [Vadrevu et al. \(2019\)](#)'s regional analysis showing precipitation as a dominant control on Indonesian fire variability—though our analysis suggests this relationship intensifies at finer spatial scales.

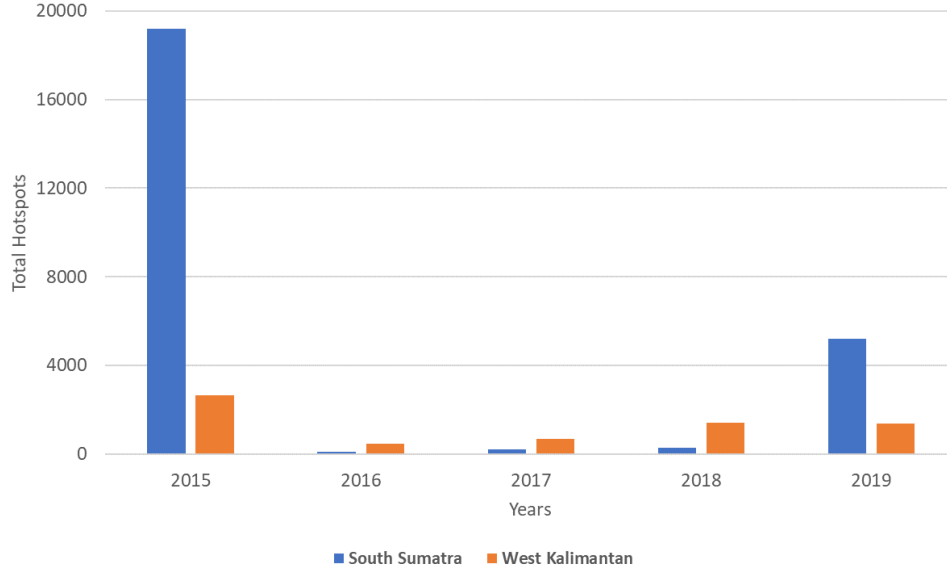


Fig. 3 Annual hotspot occurrences with confidence levels exceeding 80% for South Sumatra and West Kalimantan (2015-2019).

The 2015 and 2019 El Niño years dominated fire activity (Figure 3). The September-October 2015 fires produced catastrophic carbon emissions, with Huijnen et al. (2016) documenting daily CO₂ releases that exceeded entire nations' fossil fuel outputs. The 2019 fires, despite a weaker El Niño, generated severe PM_{2.5} pollution that Grosvenor et al. (2024) linked to substantial excess mortality across the region. These impacts demand better fire prediction.

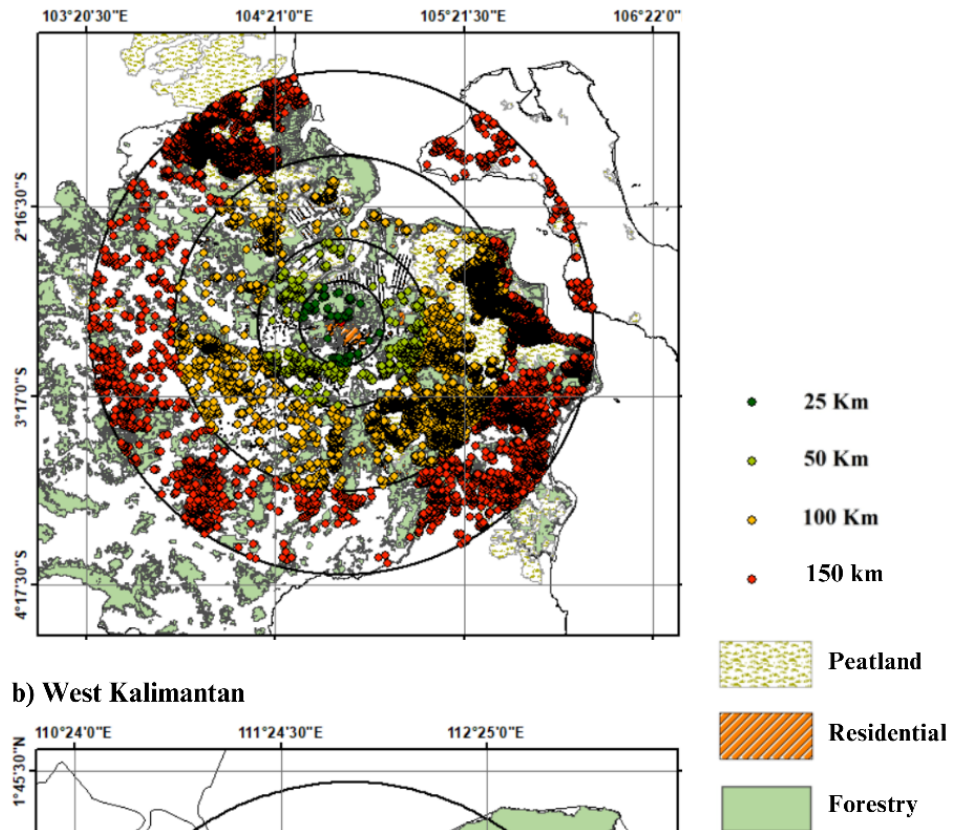
Drought duration controlled fire intensity exponentially. We classified 1,826 discrete dry periods across both provinces. Very short droughts (1-5 days) occurred most frequently—687 events in South Sumatra, 682 in West Kalimantan—but generated minimal fire activity, averaging just 2.3 ± 1.4 and 1.8 ± 1.2 hotspots per event respectively. Short droughts (6-10 days) happened less often (160 in South Sumatra, 106 in West Kalimantan) but quadrupled fire activity to 8.7 ± 3.2 and 6.4 ± 2.8 hotspots per event.

The fire response intensified dramatically with moderate droughts (11-20 days). Despite occurring only 71 times in South Sumatra and 73 times in West Kalimantan, these events averaged 24.5 ± 9.1 and 18.3 ± 7.6 hotspots respectively. Long droughts (21-30 days) proved catastrophic—though rare (27 events in South Sumatra, 11 in West Kalimantan), they generated 89.4 ± 21.3 and 72.1 ± 18.9 hotspots per event.

The provincial difference emerged starkly in extreme droughts. South Sumatra experienced 17 very long drought events exceeding 30 days, averaging 156.2 ± 34.7 hotspots each. West Kalimantan recorded zero events in this category—its maritime position and equatorial rainfall regime apparently prevent such extreme drying. This

289 fundamental hydrological difference questions whether universal drought indices can
290 adequately capture fire risk across Indonesia’s diverse landscapes, supporting [Vitolo](#)
291 [et al. \(2020\)](#)’s argument for region-specific thresholds.

a) South Sumatera



b) West Kalimantan

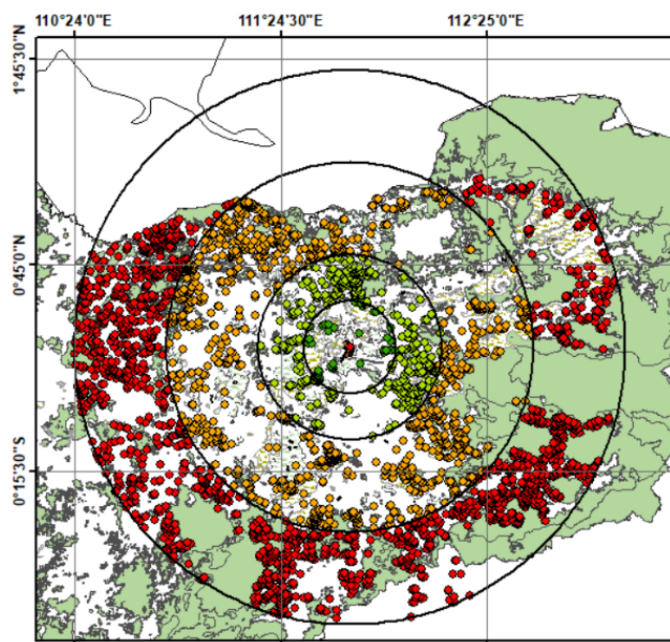


Fig. 4 Spatial distribution of hotspots across buffer zones (25, 50, 100, 150 km) overlaid on land cover types for (a) South Sumatera and (b) West Kalimantan provinces.

292 Fire distribution showed clear spatial structure (Figure 4). Within 25 km of weather
 293 stations, hotspot detection remained minimal—urban and residential land use domi-
 294 nates these areas. This matches Nikonovas et al. (2021)’s observation that urbanization
 295 creates effective firebreaks. But it creates a measurement problem: weather stations
 296 sit in fire-resistant zones while peatlands burn 50-100 km away.

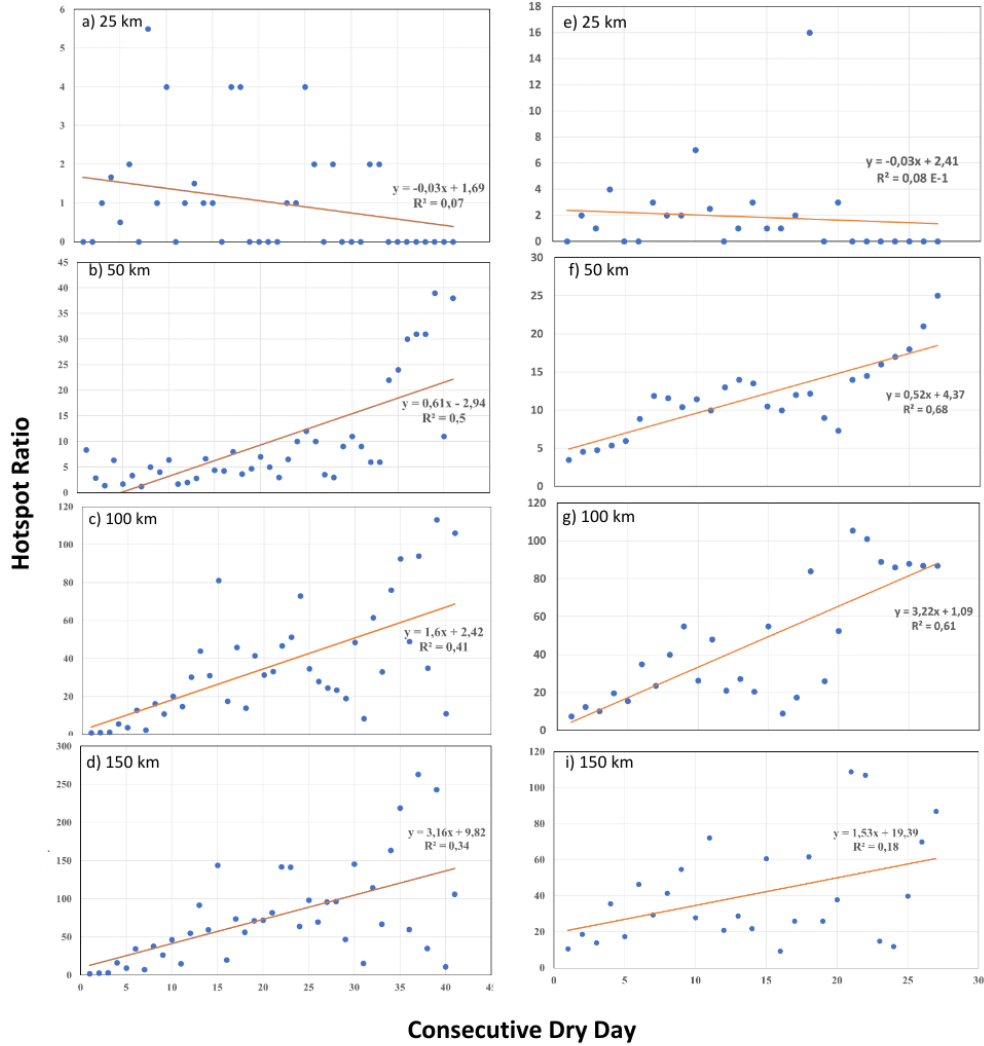


Fig. 5 Scatter plots showing correlations between CDD values and hotspot ratios at different buffer radii for South Sumatra (a-d) and West Kalimantan (e-h). Regression lines and R² values indicate relationship strength.

297 The correlation between drought and fire depended critically on spatial scale
 298 (Figure 5). At 25 km radius, correlations turned negative ($r = -0.265$ for South Sumatra, $r = -0.093$ for West Kalimantan)—urbanization near stations suppresses fire
 299 despite drought. At 50 km, correlations peaked sharply: $r = 0.776$ ($R^2 = 0.50$) for South Sumatra and $r = 0.821$ ($R^2 = 0.68$) for West Kalimantan ($p < 0.01$ for both). This 50
 300 km sweet spot aligns with ABL theory, where Rahman et al. (2021) showed tropical
 301 mixing processes create horizontal coherence at similar scales. Weather measurements
 302 remain representative at this distance.
 303

304 Beyond 100 km, correlations weakened again (Figure 6). At 150 km, mesoscale
 305 processes—sea breezes, convective complexes, topographic flows—break the connection
 306 between point measurements and area conditions (Lee and Wang, 2020). The 50
 307 km radius optimally balances spatial coverage against meteorological coherence.
 308

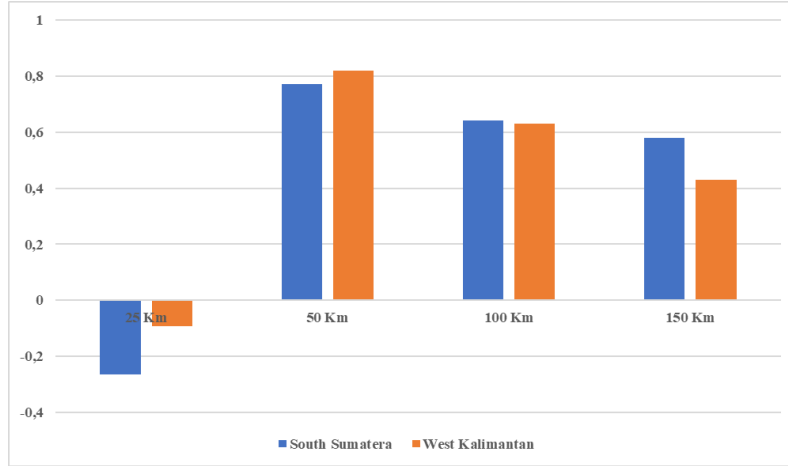


Fig. 6 Summary of Pearson correlation coefficients between CDD index and hotspot growth across buffer radii for both provinces. Error bars represent 95% confidence intervals.

309 The exponential fire response to drought duration reflects peatland hydrology.
 310 Taufik et al. (2015) documented rapid groundwater drawdown in degraded peatlands
 311 during dry periods, with critical thresholds typically crossed after several weeks with-
 312 out rain. Our data support this mechanism—very long drought events (>30 days)
 313 averaged 156.2 ± 34.7 hotspots, nearly double the 89.4 ± 21.3 hotspots from long
 314 droughts (21-30 days). Once peat ignites at depth, Li et al. (2022) showed these fires
 315 can smolder underground for extended periods, surviving even surface rainfall.

316 These findings challenge current fire management approaches. The 50 km optimal
 317 correlation distance reveals a fundamental mismatch: meteorological networks
 318 designed for aviation and agriculture miss fire-prone peatlands. Stations cluster near
 319 population centers while fires rage in remote areas. Strategic station placement in
 320 peatland-forest transition zones could transform prediction accuracy.

321 The stark differences between South Sumatra and West Kalimantan—particularly
 322 the absence of extreme droughts in the latter—argue against one-size-fits-all warning

systems. South Sumatra needs alerts calibrated to its monsoon-driven extremes, while West Kalimantan requires sensitivity to shorter but still dangerous dry spells. This aligns with [Vilchis-Francés et al. \(2021\)](#)’s demonstration that locally-tuned indices outperform global standards.

[Horton et al. \(2022\)](#) demonstrated that strategic land management can substantially reduce peatland fire occurrence, with our urban-rural gradient supporting this finding—the negative correlations at 25 km radius show how modified landscapes resist burning. Yet most peatlands lack such protection.

Looking forward, combining CDD data with satellite soil moisture could capture the nonlinear drought-fire relationship more completely. [Richardson et al. \(2022\)](#) showed multi-variable drought indices consistently outperform single metrics. Machine learning approaches might untangle the scale-dependent patterns we observed, potentially extending warning lead times. For communities facing these fires, every additional day of warning saves lives and livelihoods.

4 Conclusion

This study demonstrates that the relationship between CDD and tropical peatland fire occurrence exhibits strong scale dependency, with optimal meteorological station representativeness achieved at 50 km radius where Pearson correlations reach 0.776–0.821 ($p < 0.01$). The identified spatial scale aligns with ABL dynamics in tropical regions, where daytime mixing heights of 1–2 km create coherent meteorological conditions across 40–60 km horizontal distances. Our findings reveal critical limitations in current fire monitoring networks, where urban-biased station placement and excessive spacing (>100 km) fail to capture drought conditions in fire-prone peatland-forest interfaces. The exponential increase in fire occurrence beyond 20 CDD, coupled with province-specific drought severity patterns, indicates that universal drought thresholds poorly represent the heterogeneous fire environments across Indonesian provinces.

These results have immediate implications for improving early warning systems across Southeast Asia’s fire-prone regions, where limited meteorological infrastructure must serve vast peatland landscapes vulnerable to climate extremes. Strategic deployment of weather stations at 50 km intervals within peatland areas, combined with regionally calibrated CDD thresholds, could substantially enhance fire prediction accuracy and provide critical lead time for community evacuation and resource mobilization. Future research should integrate high-resolution satellite soil moisture data with ground observations to bridge the scale gap between point measurements and landscape-level fire dynamics, while machine learning approaches may better capture the nonlinear relationships between cumulative drought stress and deep peat ignition probability. As climate change intensifies ENSO-driven droughts across the Maritime Continent, optimizing the spatial configuration of meteorological networks represents a cost-effective adaptation strategy for reducing the catastrophic health, economic, and carbon emissions impacts of tropical peatland fires.

Acknowledgments

We gratefully acknowledge financial support from the Dean’s Distinguished Fellowship awarded by the College of Natural and Agricultural Sciences, University of California, Riverside (2023) to S.H.S.H., and from the Institut Teknologi Bandung Research, Community Service and Innovation Program (PPMI-ITB 2023: FITB.PN-6-12-2023) to R.S. We thank NASA’s Fire Information for Resource Management System (FIRMS) for providing open access to MODIS Terra and Aqua active fire data (<https://firms.modaps.eosdis.nasa.gov/>), which formed the foundation of our hotspot analysis. Meteorological station data were obtained from the Indonesian Agency for Meteorology, Climatology and Geophysics (BMKG) data portal (<https://dataonline.bmkg.go.id/>) and the OGIMET synoptic data repository (<https://www.ogimet.com/>). All primary data sources used in this study are freely accessible through these platforms. Processed datasets, including spreadsheets containing normalized hotspot ratios and ArcGIS project files with buffer analysis outputs, are available from the corresponding author upon reasonable request.

References

- Bohlmann, S., Laine, M.: Statistical calibration of probabilistic medium-range Fire Weather Index forecasts in Europe. *Natural Hazards and Earth System Sciences* **24**(12), 4225–4235 (2024) <https://doi.org/10.5194/nhess-24-4225-2024>
- Bataineh, A.L., Oswald, B.P., Bataineh, M., Unger, D., Hung, I.-K., Scognamiglio, D.: Spatial autocorrelation and pseudoreplication in fire ecology. *Fire Ecology* **2**, 107–118 (2006) <https://doi.org/10.4996/fireecology.0202107>
- Crawford, A.J., Belcher, C.M., New, S., Gallego-Sala, A., Swindles, G.T., Page, S., Blyakharchuk, T.A., Cadillo-Quiroz, H., Charman, D.J., Galka, M., Hughes, P.D.M., Lähteenoja, O., Mauquoy, D., Roland, T.P., Väliranta, M.: Tropical peat composition may provide a negative feedback on fire occurrence and severity. *Nature Communications* **15**(1), 6606 (2024) <https://doi.org/10.1038/s41467-024-50916-7>
- Chen, F., Fan, Z., Niu, S., Zheng, J.: The Influence of Precipitation and Consecutive Dry Days on Burned Areas in Yunnan Province, Southwestern China. *Advances in Meteorology* **2014**, 748923 (2014) <https://doi.org/10.1155/2014/748923>
- Cobb, A.R., Hoyt, A.M., Gandois, L., Eri, J., Dommain, R., Abu Salim, K., Kai, F.M., Haji Su’ut, N.S., Harvey, C.F.: How temporal patterns in rainfall determine the geomorphology and carbon fluxes of tropical peatlands. *Proceedings of the National Academy of Sciences* **114**(26), 5187–5196 (2017) <https://doi.org/10.1073/pnas.1701090114>
- Csiszar, I.A., Morisette, J.T., Giglio, L.: Validation of active fire detection from moderate-resolution satellite sensors: the MODIS example in northern eurasia. *IEEE Transactions on Geoscience and Remote Sensing* **44**(7), 1757–1764 (2006) <https://doi.org/10.1109/TGRS.2006.875941>

- 402 Dadap, N.C., Cobb, A.R., Hoyt, A.M., Harvey, C.F., Konings, A.G.: Satellite soil mois-
403 ture observations predict burned area in Southeast Asian peatlands. *Environmental*
404 *Research Letters* **14**(9), 094014 (2019) <https://doi.org/10.1088/1748-9326/ab3891>
- 405 Duan, Y., Ma, Z., Yang, Q.: Characteristics of consecutive dry days variations in
406 China. *Theoretical and Applied Climatology* **130**, 701–709 (2017) [https://doi.org/](https://doi.org/10.1007/s00704-016-1984-6)
407 [10.1007/s00704-016-1984-6](https://doi.org/10.1007/s00704-016-1984-6)
- 408 Edwards, R.B., Naylor, R.L., Higgins, M.M., Falcon, W.P.: Causes of Indonesia’s forest
409 fires. *World Development* **127**, 104717 (2020) [https://doi.org/10.1016/j.worlddev.](https://doi.org/10.1016/j.worlddev.2019.104717)
410 [2019.104717](https://doi.org/10.1016/j.worlddev.2019.104717)
- 411 Field, R.D., van der Werf, G.R., Fanin, T., Fetzer, E.J., Fuller, R., Jethva, H., Levy, R.,
412 Livesey, N.J., Luo, M., Torres, O., Worden, H.M.: Indonesian fire activity and smoke
413 pollution in 2015 show persistent nonlinear sensitivity to El Niño-induced drought.
414 *Proceedings of the National Academy of Sciences* **113**(33), 9204–9209 (2016) <https://doi.org/10.1073/pnas.1524888113>
415 [//doi.org/10.1073/pnas.1524888113](https://doi.org/10.1073/pnas.1524888113)
- 416 Graham, L.L.B., Applegate, G.B., Thomas, A., Ryan, K.C., Saharjo, B.H., Cochrane,
417 M.A.: A Field Study of Tropical Peat Fire Behaviour and Associated Carbon
418 Emissions. *Fire* **5**(3), 62 (2022) <https://doi.org/10.3390/fire5030062>
- 419 Grosvenor, M.J., Ardiyani, V., Wooster, M.J., Gillott, S., Graham, L.L.B., Gray, N.,
420 Remedios, J.: Catastrophic impact of extreme 2019 Indonesian peatland fires on
421 urban air quality and health. *Communications Earth & Environment* **5**, 649 (2024)
422 <https://doi.org/10.1038/s41467-024-01813-w>
- 423 Gaveau, D.L.A., Salim, M.A., Hergoualc’h, K., Locatelli, B., Sloan, S., Wooster, M.,
424 Marlier, M.E., Molidena, E., Yaen, H., DeFries, R., Verchot, L., Murdiyarso, D.,
425 Nasi, R., Holmgren, P., Sheil, D.: Major atmospheric emissions from peat fires in
426 Southeast Asia during non-drought years: evidence from the 2013 Sumatran fires.
427 *Scientific Reports* **4**, 6112 (2014) <https://doi.org/10.1038/srep06112>
- 428 Giglio, L., Schroeder, W., Justice, C.O.: The Collection 6 MODIS active fire detection
429 algorithm and fire products. *Remote Sensing of Environment* **178**, 31–41 (2016)
430 <https://doi.org/10.1016/j.rse.2016.02.054>
- 431 Hirano, T., Kusin, K., Limin, S., Osaki, M.: Evapotranspiration of tropical peat swamp
432 forests. *Global Change Biology* **21**(5), 1914–1927 (2015) [https://doi.org/10.1111/](https://doi.org/10.1111/gcb.12653)
433 [gcb.12653](https://doi.org/10.1111/gcb.12653)
- 434 Horton, A.J., Lehtinen, J., Kumm, M.: Targeted land management strategies could
435 halve peatland fire occurrences in Central Kalimantan, Indonesia. *Communications*
436 *Earth & Environment* **3**, 204 (2022) <https://doi.org/10.1038/s43247-022-00534-2>
- 437 Havlicek, L.L., Peterson, N.L.: Robustness of the Pearson correlation against violations
438 of assumptions. *Perceptual and Motor Skills* **43**(3), 1319–1334 (1976) <https://doi.org/10.1002/ps.1000>

- 439 [org/10.2466/pms.1976.43.3f.1319](https://doi.org/10.2466/pms.1976.43.3f.1319)
- 440 Hein, L., Spadaro, J.V., Ostro, B., Hammer, M., Sumarga, E., Salmayenti, R.,
 441 Boer, R., Tata, H., Atmoko, D., Castañeda, J.-P.: The health impacts of Indone-
 442 sian peatland fires. *Environmental Health* **21**, 62 (2022) [https://doi.org/10.1186/](https://doi.org/10.1186/s12940-022-00872-w)
 443 [s12940-022-00872-w](https://doi.org/10.1186/s12940-022-00872-w)
- 444 Huijnen, V., Wooster, M.J., Kaiser, J.W., Gaveau, D.L.A., Flemming, J., Parrington,
 445 M., Inness, A., Murdiyarso, D., Main, B., Weele, M.: Fire carbon emissions over
 446 maritime southeast Asia in 2015 largest since 1997. *Scientific Reports* **6**, 26886
 447 (2016) <https://doi.org/10.1038/srep26886>
- 448 Hu, Y., Yue, X., Tian, C.: Impacts of El Niño–Southern Oscillation on global fire
 449 PM_{2.5} during 2000–2023. *Atmospheric and Oceanic Science Letters* **18**(3), 100597
 450 (2025) <https://doi.org/10.1016/j.aosl.2025.100597>
- 451 Kudláčková, L., Bartošová, L., Linda, R., Bláhová, M., Poděbradská, M., Fischer, M.,
 452 Balek, J., Žalud, Z., Trnka, M.: Assessing fire danger classes and extreme thresh-
 453 olds of the Canadian Fire Weather Index across global environmental zones: a
 454 review. *Environmental Research Letters* **20**(1), 013001 (2024) [https://doi.org/10.](https://doi.org/10.1088/1748-9326/ad97cf)
 455 [1088/1748-9326/ad97cf](https://doi.org/10.1088/1748-9326/ad97cf)
- 456 Konecny, K., Ballhorn, U., Navratil, P., Jubanski, J., Page, S.E., Tansey, K., Hooijer,
 457 A., Vernimmen, R., Siegert, F.: Variable carbon losses from recurrent fires in drained
 458 tropical peatlands. *Global Change Biology* **22**(4), 1469–1480 (2016) [https://doi.](https://doi.org/10.1111/gcb.13186)
 459 [org/10.1111/gcb.13186](https://doi.org/10.1111/gcb.13186)
- 460 Koplitz, S.N., Mickley, L.J., Jacob, D.J., Marlier, M.E., DeFries, R.S., Gaveau, D.L.A.,
 461 Locatelli, B., Reid, J.S., Xian, P., Myers, S.S.: Role of the Madden-Julian Oscillation
 462 in the Transport of Smoke From Sumatra to the Malay Peninsula During Severe
 463 Non-El Niño Haze Events. *Journal of Geophysical Research: Atmospheres* **123**(11),
 464 6282–6294 (2018) <https://doi.org/10.1029/2018JD028533>
- 465 Kiely, L., Spracklen, D.V., Arnold, S.R., Papargyropoulou, E., Conibear, L., Wied-
 466 inmyer, C., Knote, C., Adrianto, H.A.: Assessing costs of Indonesian fires and
 467 the benefits of restoring peatland. *Nature Communications* **12**, 7044 (2021) [https:](https://doi.org/10.1038/s41467-021-27353-x)
 468 [//doi.org/10.1038/s41467-021-27353-x](https://doi.org/10.1038/s41467-021-27353-x)
- 469 Linn, R.R., Hiers, J.K., O'Brien, J.J., Yedinak, K., Hoffman, C., Canfield, J., Robin-
 470 son, D., Goodrick, S.: Wildland fire entrainment: The missing link between wildland
 471 fire and its environment. *PNAS Nexus* **4**(1), 576 (2025) [https://doi.org/10.1093/](https://doi.org/10.1093/pnasnexus/pgae576)
 472 [pnasnexus/pgae576](https://doi.org/10.1093/pnasnexus/pgae576)
- 473 Lee, H.-H., Wang, C.: The impacts of biomass burning activities on convective systems
 474 over the Maritime Continent. *Atmospheric Chemistry and Physics* **20**(4), 2533–2548
 475 (2020) <https://doi.org/10.5194/acp-20-2533-2020>

- Li, W., Xu, Q., Yi, J., Liu, J.: Predictive model of spatial scale of forest fire driving factors: a case study of Yunnan Province, China. *Scientific Reports* **12**, 19029 (2022) <https://doi.org/10.1038/s41598-022-23697-6>
- Marlier, M.E., DeFries, R.S., Kim, P.S., Gaveau, D.L.A., Koplitz, S.N., Jacob, D.J., Mickley, L.J., Margono, B.A., Myers, S.S.: Regional air quality impacts of future fire emissions in Sumatra and Kalimantan. *Environmental Research Letters* **10**(5), 054010 (2015) <https://doi.org/10.1088/1748-9326/10/5/054010>
- Mortelmans, J., Felsberg, A., De Lannoy, G.J.M., Veraverbeke, S., Field, R.D., Andela, N., Bechtold, M.: Improving the fire weather index system for peatlands using peat-specific hydrological input data. *Natural Hazards and Earth System Sciences* **24**(2), 445–464 (2024) <https://doi.org/10.5194/nhess-24-445-2024>
- Ma, M., Wu, Y., Luo, W., Chen, L., Li, J., Jing, N.: HiBuffer: Buffer analysis of 10-million-scale spatial data in real time. *ISPRS International Journal of Geo-Information* **7**(12), 467 (2018) <https://doi.org/10.3390/ijgi7120467>
- Nikonovas, T., Spessa, A., Doerr, S.H., Clay, G.D., Mezbahuddin, S.: Near-complete loss of fire-resistant primary tropical forest cover in Sumatra and Kalimantan. *Communications Earth & Environment* **1**, 65 (2021) <https://doi.org/10.1038/s43247-020-00069-4>
- O, S., Hou, X., Orth, R.: Observational evidence of wildfire-promoting soil moisture anomalies. *Scientific Reports* **10**(1), 1–8 (2020) <https://doi.org/10.1038/s41598-020-67530-4>
- Pan, X., Chin, M., Ichoku, C.M., Field, R.D.: Connecting Indonesian fires and drought with the type of El Niño and phase of the Indian Ocean Dipole during 1979–2016. *Journal of Geophysical Research: Atmospheres* **123**(15), 7974–7988 (2018) <https://doi.org/10.1029/2018JD028402>
- Richardson, D., Black, A.S., Irving, D., Matear, R.J., Monselesan, D.P., Risbey, J.S., Squire, D.T., Tozer, C.R.: Global increase in wildfire potential from compound fire weather and drought. *npj Climate and Atmospheric Science* **5**, 23 (2022) <https://doi.org/10.1038/s41612-022-00248-4>
- Rahman, M.A., Nugroho, D.S., Yamanaka, M.D., Kawasaki, M., Kozan, O., Ohashi, M., Hashiguchi, H., Mori, S.: Weather radar detection of planetary boundary layer and smoke layer top of peatland fire in Central Kalimantan, Indonesia. *Scientific Reports* **11**, 367 (2021) <https://doi.org/10.1038/s41598-020-79486-6>
- Squire, D.T., Richardson, D., Risbey, J.S., Black, A.S., Kitsios, V., Matear, R.J., Monselesan, D., Moore, C.S., Tozer, C.R.: Likelihood of unprecedented drought and fire weather during Australia’s 2019 megafires. *npj Climate and Atmospheric Science* **4**, 64 (2021) <https://doi.org/10.1038/s41612-021-00220-8>

- Sheldon, T.L., Sankaran, C.: The Impact of Indonesian Forest Fires on Singaporean Pollution and Health. *American Economic Review* **107**(5), 526–529 (2017) <https://doi.org/10.1257/aer.p20171134>
- Sun, C., Touge, Y., Shi, K., Tanaka, K.: Assessment of the suitability of drought descriptions for wildfires under various humid temperate climates in Japan. *Scientific Reports* **14**, 23759 (2024) <https://doi.org/10.1038/s41598-024-75563-2>
- Stull, R.B.: An Introduction to Boundary Layer Meteorology. Kluwer Academic Publishers, Amsterdam, The Netherlands (1988). <https://doi.org/10.1007/978-94-009-3027-8>
- Tangang, F., Farzanmanesh, R., Mirzaei, A., Supari, Salimun, E., Jamaluddin, A.F., Juneng, L.: Characteristics of precipitation extremes in Malaysia associated with El Niño and La Niña events. *International Journal of Climatology* **37**, 696–716 (2017) <https://doi.org/10.1002/joc.5032>
- Taufik, M., Setiawan, B.I., van Lanen, H.A.J.: Modification of a fire drought index for tropical wetland ecosystems by including water table depth. *Agricultural and Forest Meteorology* **203**, 1–10 (2015) <https://doi.org/10.1016/j.agrformet.2014.12.006>
- Tian, X.-R., Shu, L.-F., Zhao, F.-J., Wang, M.-Y., McRae, D.J.: Future impacts of climate change on forest fire danger in northeastern China. *Journal of Forestry Research* **22**(3), 437–446 (2011) <https://doi.org/10.1007/s11676-011-0185-5>
- Taufik, M., Torfs, P.J.J.F., Uijlenhoet, R., Jones, P.D., Murdiyarso, D., Van Lanen, H.A.J.: Amplification of wildfire area burnt by hydrological drought in the humid tropics. *Nature Climate Change* **7**, 428–431 (2017) <https://doi.org/10.1038/nclimate3280>
- Taufik, M., Widyastuti, M.T., Sulaiman, A., Murdiyarso, D., Santikayasa, I.P., Minasny, B.: An improved drought-fire assessment for managing fire risks in tropical peatlands. *Agricultural and Forest Meteorology* **312**, 108738 (2022) <https://doi.org/10.1016/j.agrformet.2021.108738>
- Usup, A., Hashimoto, Y., Takahashi, H., Hayasaka, H.: Combustion and thermal characteristics of peat fire in tropical peatland in Central Kalimantan, Indonesia. *Tropics* **14**(1), 1–19 (2004) <https://doi.org/10.3759/tropics.14.1>
- Vitolo, C., Di Giuseppe, F., Barnard, C., Coughlan, R., San-Miguel-Ayanz, J., Libertá, G., Krzeminski, B.: ERA5-based global meteorological wildfire danger maps. *Scientific Data* **7**, 216 (2020) <https://doi.org/10.1038/s41597-020-0554-z>
- Vilchis-Francés, A.Y., Díaz-Delgado, C., Becerril-Piña, R., Mastachi-Loza, C.A., Gómez-Albores, M.Á., Bâ, K.M.: Daily prediction modeling of forest fire ignition using meteorological drought indices in the Mexican highlands. *iForest - Biogeosciences and Forestry* **14**(5), 437–446 (2021) <https://doi.org/10.3832/ifer3623-014>

- 550 Vadrevu, K.P., Lasko, K., Giglio, L., Schroeder, W., Biswas, S., Justice, C.: Trends in
551 Vegetation fires in South and Southeast Asian Countries. *Scientific Reports* **9**, 7422
552 (2019) <https://doi.org/10.1038/s41598-019-43940-x>
- 553 van der Werf, G.R., Randerson, J.T., Giglio, L., van Leeuwen, T.T., Chen, Y., Rogers,
554 B.M., Mu, M., van Marle, M.J.E., Morton, D.C., Collatz, G.J., Yokelson, R.J.,
555 Kasibhatla, P.S.: Global fire emissions estimates during 1997-2016. *Earth System*
556 *Science Data* **9**(2), 697–720 (2017) <https://doi.org/10.5194/essd-9-697-2017>
- 557 Werth, P.A., Potter, B.E., Clements, C.B., Finney, M.A., Goodrick, S.L., Alexan-
558 der, M.E., Cruz, M.G., Forthofer, J.A., McAllister, S.S.: Synthesis of Knowledge of
559 Extreme Fire Behavior: Volume I for Fire Managers. USDA, Forest Service, Pacific
560 Northwest Research Station, Portland, OR, USA (2011). [https://doi.org/10.2737/](https://doi.org/10.2737/pnw-gtr-854)
561 [pnw-gtr-854](https://doi.org/10.2737/pnw-gtr-854)
- 562 Yokelson, R.J., Saharjo, B.H., Stockwell, C.E., Putra, E.I., Jayarathne, T., Akbar, A.,
563 Albar, I., Blake, D.R., Graham, L.L.B., Kurniawan, A., Meinardi, S., Ningrum, D.,
564 Nurhayati, A.D., Saad, A., Sakuntaladewi, N., Setianto, E., Simpson, I.J., Stone,
565 E.A., Sutikno, S., Thomas, A., Ryan, K.C., Cochrane, M.A.: Tropical peat fire
566 emissions: 2019 field measurements in Sumatra and Borneo and synthesis with
567 previous studies. *Atmospheric Chemistry and Physics* **22**(15), 10173–10194 (2022)
568 <https://doi.org/10.5194/acp-22-10173-2022>
- 569 Zheng, H., Xue, L., Ding, K., Lou, S., Wang, Z., Ding, A., Huang, X.: ENSO-Related
570 Fire Weather Changes in Southeast and Equatorial Asia: A Quantitative Evaluation
571 Using Fire Weather Index. *Journal of Geophysical Research: Atmospheres* **128**(21),
572 2023–039688 (2023) <https://doi.org/10.1029/2023JD039688>
- 573 Zwiers, F.W., Zhang, X.: Guidelines on analysis of extremes in a changing climate
574 in support of informed decisions for adaptation. Climate Data and Monitoring,
575 WCDMP-No. 72, WMO-TD No. 1500, 56 (2009). [https://library.wmo.int/idurl/4/](https://library.wmo.int/idurl/4/48826)
576 [48826](https://library.wmo.int/idurl/4/48826)